

The Recently-Discovered Dwarf Nova System A SAS  
J002511+1217.2: A New WZ Sagittae Star<sup>1</sup>

M. R. Templeton<sup>2</sup>, R. Leaman<sup>3</sup>, P. Szkody<sup>3</sup>, A. Henden<sup>2;4</sup>, L. Cook<sup>5</sup>, D. Starkey<sup>2</sup>, A. Oksanen<sup>6</sup>, M. Koppelman<sup>2</sup>, D. Boyd<sup>7</sup>, P. R. Nelson<sup>8</sup>, T. Vanmunster<sup>9</sup>, R. Pickard<sup>10</sup>, N. Quinn<sup>11</sup>, R. Huziak<sup>2</sup>, M. Aho<sup>6</sup>, R. James<sup>2</sup>, A. Golovin<sup>12</sup>, E. Pavlenko<sup>13</sup>, R. J. Durkee<sup>14</sup>, T. R. Crawford<sup>2;15</sup>, G. Walker<sup>2</sup>, & P. P. Aakkonen<sup>16</sup>

ABSTRACT

The cataclysmic variable A SAS J002511+1217.2 was discovered in outburst by the All-Sky Automated Survey in September 2004, and intensively monitored by AA VSO observers through the following two months. Both photometry and spectroscopy indicate that this is a very short-period system. Clearly defined superhumps with a period of 0:05687 ± 0:00001 (1-σ) days (81.9 minutes) are

---

<sup>2</sup>AA VSO, 25 Birch Street, Cambridge, MA 02138

<sup>3</sup>Department of Astronomy, University of Washington, Box 351580, Seattle, WA 98195

<sup>4</sup>Universities Space Research Association/US Naval Observatory, P.O. Box 1149, Flagstaff, AZ 86002-1149

<sup>5</sup>Center for Backyard Astrophysics { Concord, 1730 Helix Ct., Concord, CA 94518

<sup>6</sup>Nyrola Observatory, K yllikinkatu 1, FI-40100 Jyväskylä, Finland

<sup>7</sup>British Astronomical Association Variable Star Section, West Challow, OX12 9TX, United Kingdom

<sup>8</sup>RM B 2493, Ellinbank, Victoria 3820, Australia

<sup>9</sup>CBA Belgium Observatory, Walhostraat 1A, B-3401 Landen, Belgium

<sup>10</sup>British Astronomical Association Variable Star Section, 3 The Birches, Shobdon, Leominster, Herefordshire HR6 9NG, England

<sup>11</sup>British Astronomical Association Variable Star Section, Steyning, West Sussex, BN44 3LR, England

<sup>12</sup>Kyiv National Shevchenko University, Physics Department; Visiting Astronomer, Crimean Astrophysical Observatory, Komunarov 63, # 39, Berdyansk, Zaporozhshka ja, 71118, Ukraine

<sup>13</sup>Crimean Astrophysical Observatory, Nauchny, Crimea, 98409, Ukraine

<sup>14</sup>Shed of Science Observatory, 5213 Washburn Ave S., Minneapolis, MN 55410

<sup>15</sup>Arch Cape Observatory, Arch Cape, OR

<sup>16</sup>Amateur Astronomer Association Seulasety, University of Joensuu, P.O. Box 111, FI-80101 Joensuu, Finland

present during the superoutburst, 5 to 18 days following the A SAS detection. We observe a change in superhump profile similar to the transition to "late superhumps" observed in other short-period systems; the superhump period appears to increase slightly for a time before returning to the original value, with the resulting superhump phase offset by approximately half a period. We detect variations with a period of  $0.05666 \pm 0.00003$  (1- $\sigma$ ) days (81.6 minutes) during the four-day quiescent phase between the end of the main outburst and the single echo outburst. Weak variations having the original superhump period reappear during the echo and its rapid decline. Time-resolved spectroscopy conducted nearly 30 days after detection and well into the decline yields an orbital period measurement of  $82 \pm 5$  minutes. Both narrow and broad components are present in the emission line spectra, indicating the presence of multiple emission regions. The weight of the observational evidence suggests that A SAS J002511+1217.2 is a WZ Sge-type dwarf nova, and we discuss how this system fits into the WZ classification scheme.

Subject headings: stars: variables: cataclysmic variables

## 1. Introduction

On 2004 September 11, the All-Sky Automated Survey (Pojmanski 2002) detected the transient object A SAS J002511+1217.2 (R.A.: 00h 25m 11.4s, Dec: +12° 17' 14.3", J2000), a source not previously known to be variable (see Price et al. (2004) for details). It was later found that the object at this position had previously been detected by ROSAT (1RXS J002510.8+121725; Voges et al. (1999)) and had been identified as a blue point source in the Hamburg Quasar Survey (Zickgraf et al. 2003). Amateur and professional astronomers from around the world began observing this object, and tracked its behavior for two months following the initial detection. Time-series spectra of A SAS J002511+1217.2 were obtained late in the outburst on JD 2,453,288 (2004 October 10) using the Apache Point Observatory 3.5-meter telescope. The spectra, obtained over a span of two hours, show radial velocity variations consistent with an orbital period of approximately 82 minutes. The photometric and spectroscopic behavior of this object is clearly that of a dwarf nova system, having many of the hallmarks of the small class of WZ Sagittae stars (Gobvin et al. 2005). The WZ Sge

---

<sup>1</sup>Based in part on observations obtained with the Apache Point Observatory (APO) 3.5m telescope, which is owned and operated by the Astrophysical Research Consortium (ARC).

stars are characterized by large-amplitude, infrequent outbursts, orbital periods below the period gap (around 2 hours), the presence of superhumps in the light curve, echo outbursts, and a slow decline from maximum light to quiescence. For an overview of the W Z Sge class, see Warner (1995).

In this paper, we discuss the available photometric and spectroscopic evidence and justify our classification of AAS J002511+1217.2 as a W Z Sge star. In Section 2, we describe the photometric observations obtained by AA VSO observers during the 2004 outburst and discuss the periodic behavior seen. In Section 3, we describe the spectroscopic observations, and the orbital parameters derived from these data. In Section 4, we discuss how this star fits into the W Z Sge class, and what questions remain about its nature.

## 2. Photometry

The photometric observations of AAS J002511+1217.2 were first discussed by Golovin et al. (2005), and were obtained during the course of the outburst beginning on 2004 September 10. Amateur and professional observers from around the world contributed nearly 17000 positive observations of AAS J002511+1217.2 between 2004 September 15 (JD 2,453,264) and 2004 December 12 (JD 2,453,352). In addition, a few hundred visual and CCD "fainter than" estimates were obtained through 2005 February 13 (JD 2,453,414.5). The majority of observations were made with CCD cameras, both filtered and unfiltered. Figure 1 shows the overall light curve of this variable, including all of the positive visual observations and un-calibrated CCD measurements. Of particular interest are the high amplitude of the initial superoutburst (nearly seven magnitudes), the early, abrupt decline in the superoutburst at JD 2,453,277 followed by a single echo outburst at JD 2,453,282, and the long decay time to quiescence (90 days). The high outburst amplitude, long decay time, and echo outbursts are phenomena observed in the W Z Sge stars, and are our primary reasons for suggesting the W Z Sge classification.

In the following subsections, we discuss the photometric behavior both early and late in the outburst, concentrating on CCD observations made early in the outburst to detect and characterize the superhump period and evolution. We also discuss the late-outburst photometry, the decline toward quiescence and the probable quiescent level.

## 2.1. Early outburst: superhumps

The photometric data were obtained by many amateur and professional observers worldwide, and were taken with a variety of equipment including telescopes of both large and small aperture, and with a variety of filters and CCD cameras. However, for period-searching the absolute calibration of the data is not very important. Therefore, prior to time-series analysis, a simple linear fit was subtracted from each observer's data on each night to remove the much larger variation of the underlying outburst along with any zero point differences. The detrended light curve of the superhumps is shown in Figure 2. As we discuss below, our time-series analysis indicates a superhump period of 0.0569 days (81.9 minutes). We do not detect any eclipse signature in the lightcurve, and any signal caused by orbital variation would be difficult to disentangle from the superhump and its evolution. For now, we treat these data as if the signal were purely due to superhumps.

### 2.1.1. Fourier analysis

Because the periods and light curve profiles of superhumps are known to change throughout the course of outbursts, we investigated whether or not period and superhump profile variations were apparent in the light curve of *ASAS J002511+12172*. We performed two separate Fourier analyses on the data: one in which we analyzed single days of photometry individually, and one in which we analyzed clusters of frequencies in the full data set's Fourier transform, to search for time-varying periods in the complete set of data. Signals with time-varying periods will generate clusters of frequencies in a Fourier power spectrum, rather than a single peak at the main frequency, and analysis of these clusters can provide information on the period evolution with time. See Foster (1995) for a description of this method.

Figure 3 shows the period as a function of time for the two analysis methods. Because the photometric coverage of individual days was not uniform, the error bars of the daily period measurements differ throughout. However, the period clearly varies at the 3 $\sigma$  level. Variations were strongly detected by the first reported time-series observations on JD 2,453,264, nine days after the outburst was first detected. Fourier analysis indicates an average period of 0.0569 days, which remained reasonably constant until JD 2,453,268 (nine days after the outburst detection) when the period began to increase by a small but significant amount.

### 2.1.2. (O-C) analysis

We also used (O-C) analysis to study the time-varying nature of the superhumps. The (O-C) method has been used in the past to study superhump evolution in SU UMa- and WZ Sge-type objects, and often shows substantial changes over the course of individual outbursts (Howell et al. 1996; Patterson et al. 2002). Figure 4 shows an (O-C) diagram of the outburst prior to the rapid decline and first echo, using an ephemeris period of 0.0569 days. Between JD 2,453,269 and 2,453,272 the phases of the superhumps steadily shifted until they reached a steady offset of approximately 0.03 days, or slightly more than half a period. This could indicate either a true change in period (Olech et al. 2004), or a change in superhump morphology. This is a common feature of dwarf novae that exhibit superhumps in outburst, and the (O-C) diagram is reminiscent of those of WZ Sge (Patterson et al. 2002) and AL Com (Howell et al. 1996). Visual inspection of Figure 2 shows that the superhumps are clearly changing in shape and amplitude as the outburst progresses.

Unfortunately, we do not have any time-series observations for the earliest part of the outburst, and thus cannot make any statement on whether so-called "orbital humps" having the orbital period were present. WZ Sge exhibited clear orbital humps during the first 12 days of the 2001 outburst, as did AL Com for the first several days. Both stars were caught very close to the outburst onset, and time-series photometry commenced immediately. There was a lag of at least five (and perhaps as much as ten) days between the onset of the outburst of AAS J002511+1217.2 and the commencement of time-series photometry. An answer to this question will have to wait until the detection of the next outburst of this system.

### 2.2. Early decline

The system began to fade rapidly after JD 2,453,276.5, and spent nearly four days at  $V = 15$  prior to the single echo outburst. The detrended time-series measurements of AAS J002511+1217.2 over this four day span are shown in Figure 5, and a Fourier spectrum of these data is shown in Figure 6. Just prior to the end of the main superoutburst, the amplitude of the superhumps dropped significantly, and they do not appear in the light curve during rapid fading. If superhumps are caused by distortion of the accretion disk (Patterson et al. 2002), then the decreasing amplitude may indicate the return of the disk to its normal shape prior to the disk transitioning from its hot, outburst state to the cool state.

A new photometric period of 0.05666 ± 0.00003 days appears in the data during its time at  $V = 15$ , and the variations have a much smoother, double-peaked profile that is quantitatively different from that of the superhumps. If this new period were the true orbital

period, the resulting period excess  $= (P_{sh} - P_{orb})/P_{orb}$  would be 0.004, smaller than that of the shortest-excess W Z Sge star EG Cnc with  $= 0.007$  (Hellier 2001). We therefore suspect that this period is not the orbital period, but is another modulation related to superhumps, and that the as-yet undetected orbital period may be closer to the period minimum.

### 2.3. Echo outburst

One echo outburst occurred approximately five days after the end of the main outburst, during which the star returned to  $V = 12.8$  for less than one day before it rapidly declined to  $V = 16$ . Following this single echo, no other echoes were observed, and AASAS J002511+1217.2 began its slow decline to quiescence over the following 70 days. Very weak variations are present during the echo; a period of about 0.0568 days is marginally detected, close to the period of the late superhumps. Golovin et al. (2005) fit maxima to these variations and integrated them into their (O-C) analysis, indicating that the resulting (O-C) is similar to that of other W Z Sge-star outbursts like W Z Sge itself (Patterson et al. 2002).

The timing of the echo outburst is similar to that of EG Cnc, which underwent a series of echo outbursts beginning several days after the initial decline of the superoutburst. However, AASAS J002511+1217.2 exhibited only one echo. There are several theories as to the causes of echo outbursts, though all theories predict that the disk must be heated over the thermal instability limit for a new outburst to occur. The occurrence of only one echo suggests that the accretion disk had either been significantly drained of matter following the initial superoutburst or first echo, or had been cooled sufficiently that the reheating mechanism could only increase the temperature beyond the instability limit one time before the disk began a transition back to its quiescent state. We discuss these scenarios further in Section 4.

### 2.4. Late outburst and return to quiescence

The end of the first echo on JD 2,453,284 left AASAS J002511+1217.2 at  $V = 16$ , and the system never rebrightened significantly over the following two months. Time-series measurements were obtained through JD 2,453,303, with visual and CCD monitoring continuing through early 2005. The system declined by about one magnitude over the 70 days following the end of the echo outburst, returning to quiescence at  $V = 17$ . A few nights of time-series CCD photometry were obtained by several observers following the echo outburst. We performed a Fourier analysis of the data, and found a signal at 0.0570 days, nearly the same

as the superhump period, and not the supposed orbital period as one would expect. This suggests that the disk remained elliptical throughout outburst and quiescence. Permanent superhumps are believed to be a feature of high mass-transfer systems, because the disk maintains a large enough radius to be tidally distorted and precessing (Osaki 1996; Retter & Naylor 2000). However, the WZ Sge stars are believed to have a low mass-transfer rate. Trampusch et al. (2005) recently found an SU UMa-type system with what appeared to be negative superhumps at quiescence, possibly due to a tilted accretion disk. Photometry of AAS J002511+1217.2 obtained with a larger telescope during quiescence can determine whether superhumps are actually present, and whether there are orbital variations.

### 3. Spectroscopy

The spectroscopic data were acquired with the Apache Point Observatory (APO) 3.5m telescope on the night of 2004 October 10 from 04:39:21 to 06:39:36 UT (JD 2,453,288.6940 to 2,453,288.7775). A total of 15 exposures were taken over this time interval, each with an exposure time of 360 seconds. This allowed observations at an average separation of seven minutes. The primary instrument used was the Double Imaging Spectrograph (DIS) run in high resolution mode with a 1.5" slit. The DIS instrument is designed so that the incoming light is split by a dichroic, and red and blue spectra are taken simultaneously on two separate CCD cameras, allowing for an extended spectral range and improved wavelength resolution. The wavelength coverage was 3850 Å to 5550 Å with 0.6 Å per pixel resolution on the blue images, and 5550 Å to 7250 Å with 0.8 Å per pixel resolution on the red images. The spectral coverage provides adequate sampling of several strong emission lines.

The raw spectra were processed using IRAF<sup>2</sup> subroutines to produce one-dimensional wavelength and flux calibrated spectra in both wavelength regimes. The target exposure time of 6 minutes allowed for reasonable signal-to-noise ratios (S/Ns) such that our orbital period uncertainties were not limited by the raw data resolution, but by limits imposed by the total span of observations and the separation interval of consecutive exposures. A V magnitude of 16.3 was estimated from the flux-calibrated spectra; this agrees with the V-band time-series photometry obtained on JD 2,453,285 and 2,453,290. Coincident R-band time-series photometry obtained around JD 2,453,288.7 has an average near 15.9.

---

<sup>2</sup>Image Reduction and Analysis Facility, is distributed by the National Optical Astronomy Observatories, which are operated by the Association of Universities for Research in Astronomy, Inc., under cooperative agreement with the National Science Foundation.

### 3.1. Spectroscopic results

Figure 7 shows sample red and blue spectra for A SA S J002511+ 1217 2. All the spectra show prominent, broad Balmer lines in emission with a central absorption that is typical for systems containing an accretion disk. The average equivalent widths were 66, 39, and 24 Å for H $\gamma$ , H $\beta$  and H $\alpha$  respectively. These values, together with the widths of the line (full-width, zero-intensity measures of 75 Å and 60 Å for H $\alpha$  and H $\beta$  respectively) and the depth of the central absorption imply a fairly high inclination.

Velocity measurements of the Balmer emission lines were made in order to determine the orbital period of the system. The H $\gamma$ , H $\beta$ , and H $\alpha$  lines all had sufficient signal to noise to allow for measurement of their central wavelengths. Initially, the IRAF centroid fitting technique 'c' was used in the splot task to estimate the line wavelengths in each spectrum over the course of the night. These wavelengths together with observation times were run through the IDL routine sinfit3 that performed a least-squares sinusoidal fit to the data, and simultaneously output the calculated values and uncertainties for period (P), semi-amplitude (K), phase offset ( $\phi$ ) and the velocity of the system ( $v$ ). However, as one example shows in Figure 8, some of the lines had sub-structure that prevented a consistent wavelength estimate. Although the emission lines were strong and statistically distinguishable from the continuum noise, narrow components can distort the centroid calculation.

A second velocity measurement was made of all spectra using a double Gaussian routine that is optimized to measure the line wings (Shaffer 1983). This method works best for broad lines with high signal to noise ratios. Shaffer found that the optimum Gaussian separation width for computing the central wavelength corresponds to an effective flux of about  $\langle f \rangle = 0.3$  or  $\frac{1}{3}$  of the line flux. Analyzing the velocities closer to the wings of the emission lines rules out the possibility that variations resulting from a hotspot located in the outer edge of the disk could mislead a centroid finding program, as the wings correspond to the faster rotating inner disk. To allow maximum flexibility for a variety of spectra, this method iterates through and produces a variety of Gaussian separations as a function of velocity. Each one of these Gaussian separations is put into the IDL routine sinfit which generates a radial velocity curve where the errors can be minimized interactively. By looking at a diagnostic plot (Figure 9) of the sinusoidal fits for each of the radial velocity measurements, the fit with the lowest errors could be selected for each of the emission lines. The best estimate for the period from this Double Gaussian method, could then be set as a fixed parameter in our original IDL sinusoidal fitting routine (sinfit3) and the error estimates could be compared with an unconstrained fit. Additional analysis attempting to search for periodicity in the blue and red continuum fluxes in the spectra showed no repetitive behavior.

The final parameters from both of the analysis routines are presented for comparison in Table 1. Since there was large disagreement in the periods for the centroid analysis (which could be partly due to the differing contributions of the narrow line component in the blue versus the red), we fixed the period at the average of the Double Gaussian method for the 3 lines (82 m in) and reran a final solution which is the bottom entry in Table 1. The fits to the data with this solution are shown in Figure 10.

An analysis of the narrow components of the Balmer emission features via the same IRAF centroid routine was attempted to estimate the location of a hotspot. The phase offset between the narrow and broad components allows us to quantitatively estimate where the mass stream impacts the accretion disk. However, measurement of the narrow component is difficult as it could not be accurately located at all phases. The result of our measurements of the velocities for the narrow component in H $\beta$  is shown overplotted with the broad component in Figure 11.

Although an exact origin of the narrow component cannot be calculated, the narrow component is most visible around an orbital phase of 0.9. This rules out irradiation of the secondary star as an origin for this component, because at an orbital phase of 0.9 the secondary is near inferior conjunction and we are viewing the side of the secondary that is away from the white dwarf. This, together with the phase offset and large velocity amplitude of the narrow component (Figure 11) argues for an origin in a hot spot due to the impact of the accretion stream on the outer edge of the disk.

#### 4. A SAS J002511+1217.2: A new WZ Sge system

We argue that the observational evidence gathered so far indicates that A SAS J002511+1217.2 is a WZ Sge star. The outburst amplitude of seven magnitudes (based upon the initial A SAS detection at V 10:4 and the Hamburg Quasar Survey pre-outburst detection at V 17:3) is marginally larger than the maximum of about six magnitudes seen in SU UMa-type dwarf novae. This star is also a 2MASS point source, and the (J - H) and (H - K) colors of 0:729 - 0:239 and 0:357 - 0:292 respectively suggest a late-K, early-M companion (see Figure 4 in Hoard et al. (2002)). The period as derived from superhumps and late-outburst photometry is short, and similar to other known WZ Sge systems, although SU UMa stars can have similarly short periods. The superhump evolution is nearly identical to that observed in other WZ Sge stars. The overall outburst lightcurve is similar to those of WZ Sge systems, including the presence of an echo outburst, and a very long decay time to true quiescence (at least 90 days from peak to V 17). The echo outburst is particularly striking evidence, as echoes have not been detected in SU UMa stars; only in WZ Sge stars. The single echo

detected in A S A S J002511+ 1217.2 was separated by a few days from the rapid decline of the main outburst, as is seen in the most prominent echo outburster, EG Cnc.

However, further information is needed since we lack a clear understanding of the development of the superhumps, and haven't determined the orbital period. The period of  $0.05666 \pm 0.00005$  days observed during the short quiescent interval between the main outburst and the first echo is accurate, and does not appear to be a sidelobe misidentification. The 0.0570-day period present after JD 2,453,288 matches the supposed superhump period observed during the main outburst. It is possible that the early variations observed during the main outburst were orbital humps, before the disk had begun to precess, but such humps typically appear very early in outburst. Our time-series photometry does not begin until at least five days after the star reached maximum, and it is possible that the true maximum occurred as much as five days before the A S A S detection because the last non-detection was made on JD 2,453,254.

The presence of only one echo outburst may indicate a low mass transfer rate. Echo outbursts may be due to several things, including a temporary increase in mass transfer caused by heating of the secondary (Patterson et al. 1998; Buat-Ménard & Hamery 2002), or temporary reheating episodes of a still-elliptical, post-superoutburst disk while it drains (Schreiber & Gansicke 2001; O saki, Meyer, & Meyer-Hofmeister 2001; Matthews et al. 2005). The presence of superhumps during echo outbursts that are in phase with those of the main outburst (Golovin et al. 2005) suggests that the main outburst ends while the disk is still elliptical. If echo outbursts are triggered by mass draining from the outer disk, then the single echo implies that this reservoir was sufficiently drained by the original outburst and first echo to preclude any additional echoes.

## 5. Conclusions

Our photometric and spectroscopic study of A S A S J002511+ 1217.2 has revealed a system showing all the properties of a low accretion rate dwarf nova. The bulk of the evidence (large outburst amplitude, an echo outburst, superhumps, long decline to quiescence, and a suspected short orbital period) justifies a W Z Sge classification rather than an SU UMa system. It does not appear that this system has eclipses, although the breadth and deep doubling of the emission lines implies a fairly high inclination. Longer time-resolved spectroscopy can be used to pin down the orbital period to higher precision. This can then be compared with the superhump period to obtain a period excess and hence a mass ratio and estimate of the mass of the secondary, as has been done for other W Z Sge systems (Patterson et al. 1998). Further time-resolved photometry during quiescence can determine if

the continuum is modulated at the orbital period due to structures in the disk. Continued monitoring of this system, both by the amateur community and by automated systems such as AASAS (Pojmanski 2002) can catch future outbursts and determine if the single echo outburst is typical of this system, and related to its particular mass transfer rate. This system is bright enough at maximum to be well within the range of both visual and CCD observers.

We acknowledge with thanks the variable star observations from the AAVSO International Database contributed by observers worldwide and used in this research. PS acknowledges support from NSF grant AST 02-05875. The AAVSO thanks the Curry Foundation for their continued support of the AAVSO International High-Energy Network. This publication makes use of data products from the Two Micron All Sky Survey, which is a joint project of the University of Massachusetts and the Infrared Processing and Analysis Center/California Institute of Technology, funded by the National Aeronautics and Space Administration and the National Science Foundation.

#### REFERENCES

- Buat-Ménard, V. & Hamery, J.M. 2002, *A & A*, 386, 891
- Foster, G. 1995, *A J*, 109, 1889
- Golovin, A. et al. 2005, *IBVS* 5611
- Hellier, C. 2001, *PASP*, 113, 469
- Hoard, D.W. et al. 2002, *ApJ*, 565, 511
- Howell, S.B., et al., 1996, *A J*, 111, 2367
- Matthews, O.M. et al. 2005, in *The Astrophysics of Cataclysmic Variables and Related Objects*, J.M. Hamery and J.P. Lasota, eds. (San Francisco: ASP)
- Olech, A. et al. 2004, *Acta Astron.*, 54, 233
- Otsuki, Y. 1996, *PASP*, 108, 39
- Otsuki, Y., Meyer, F., & Meyer-Hofmeister, E. 2001, *A & A*, 370, 488
- Patterson, J., et al., 1998, *PASP*, 110, 1290
- Patterson, J., et al., 2002, *PASP*, 114, 721

Pojnanski, G., 2002, *Acta Astron.*, 52, 397

Price, A., et al. 2004, *IAUC* 8410, 1

Reiter, A. & Naylor, T. 2000, *MNRAS*, 319, 510

Schreiber, M. R. & Gansicke, B. T. 2001, *A & A*, 375, 937

Shaffer, A. W., 1983, *ApJ*, 267, 222

Tramposch, J. et al. 2005, *PASP*, 117, 262

Voges, W., et al., 1999, *A & A*, 349, 389

Wamer, B., 1995, *Cataclysmic Variable Stars* (New York: Cambridge University Press)

Zickgraf, F.-J., Engels, D., Hagen, H.-J., Reimers, D. & Voges, W., 2003, *A & A*, 406, 535

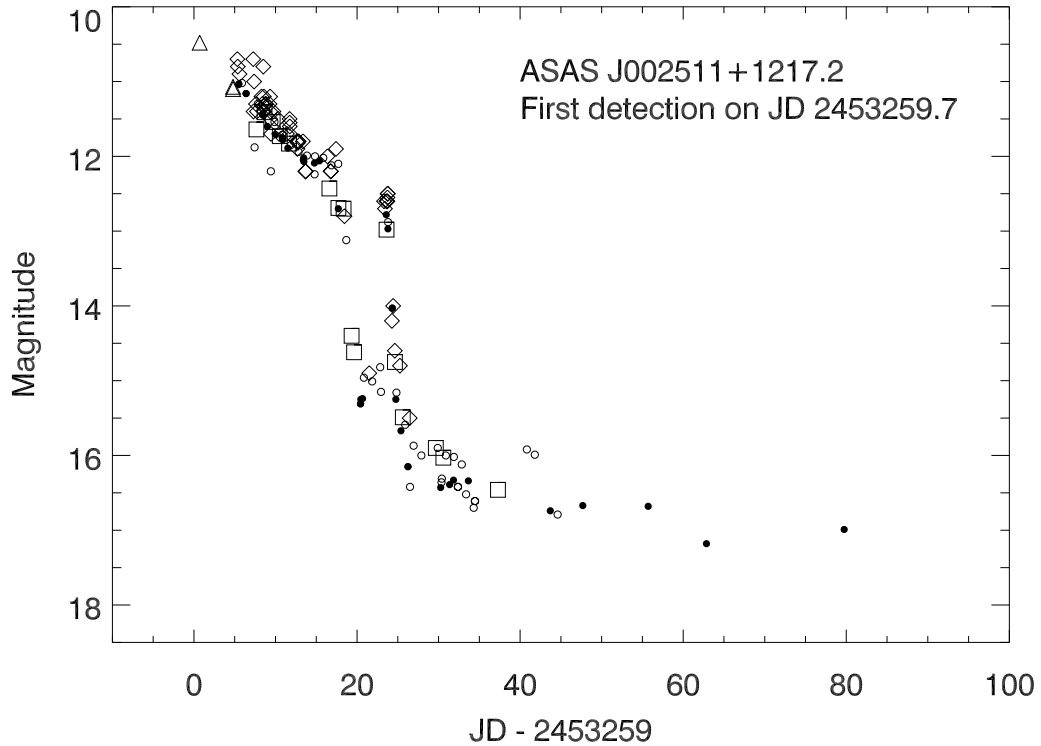


Fig. 1. | Outburst light curve of ASAS J002511+1217.2. The outburst amplitude is nearly seven magnitudes from the presumed quiescent level of  $V = 17.3$ . The main "superoutburst" lasted for at least 18 days, and one echo outburst was observed approximately 5 days after the initial outburst ended. Following the echo outburst, the star dropped below  $V = 16$ , and slowly faded to  $V = 17$  through the end of 2004. The data points are nightly averages of individual observers (CCD observations) or individual visual estimates. Open diamonds: visual magnitude estimates; open circles: unfiltered CCD observations; filled circles: V-band CCD observations; open squares: R-band CCD observations; open triangles: ASAS V-band observations. We note that the data are not on a common photometric system, and some of the variations are due to observer-to-observer zero-point differences of a few tenths of a magnitude. This is particularly the case with unfiltered CCD observations, where the spectral response of individual observers' systems can vary widely. All linear trends and zero-point differences are subtracted from individual observers' nightly time-series data prior to analysis.

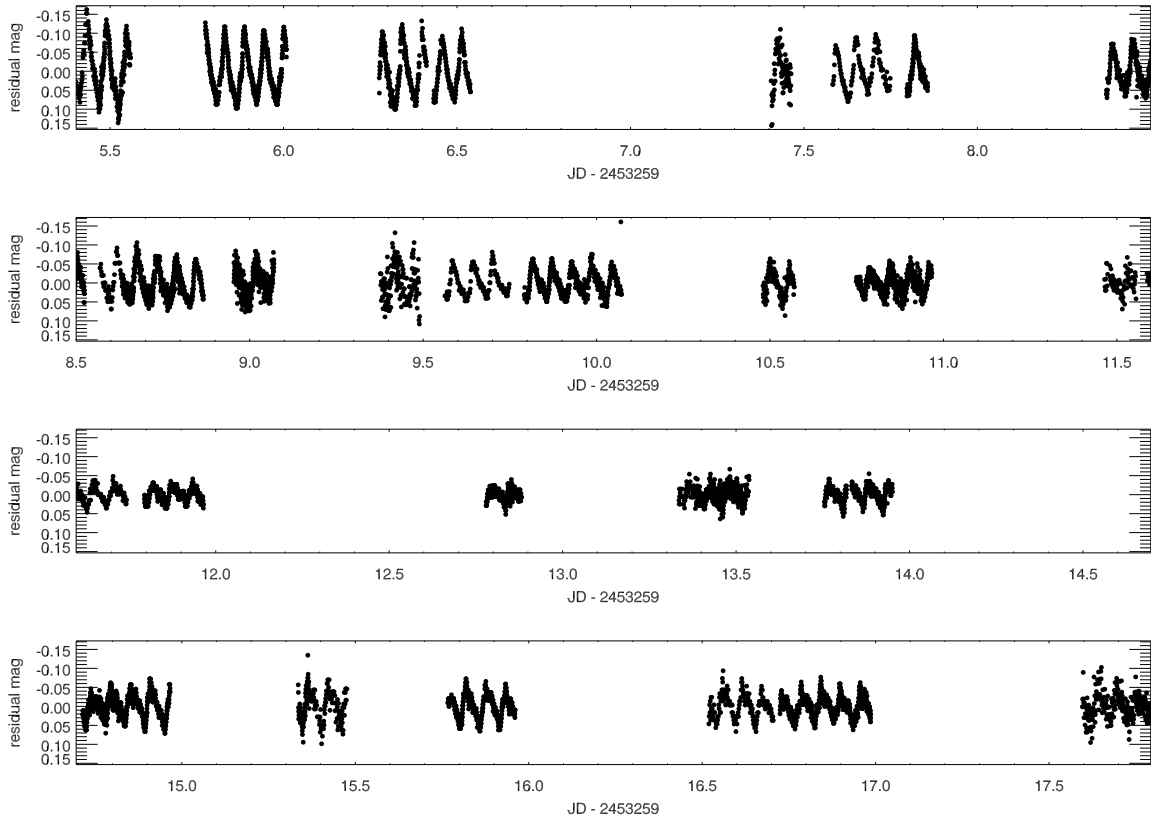


Fig. 2. Superhump light curve of A SA S J002511+12172 from JD 2,453,264 to 2,453,276. The light curve shows significant evolution of the superhump profile and amplitude over the course of the outburst.

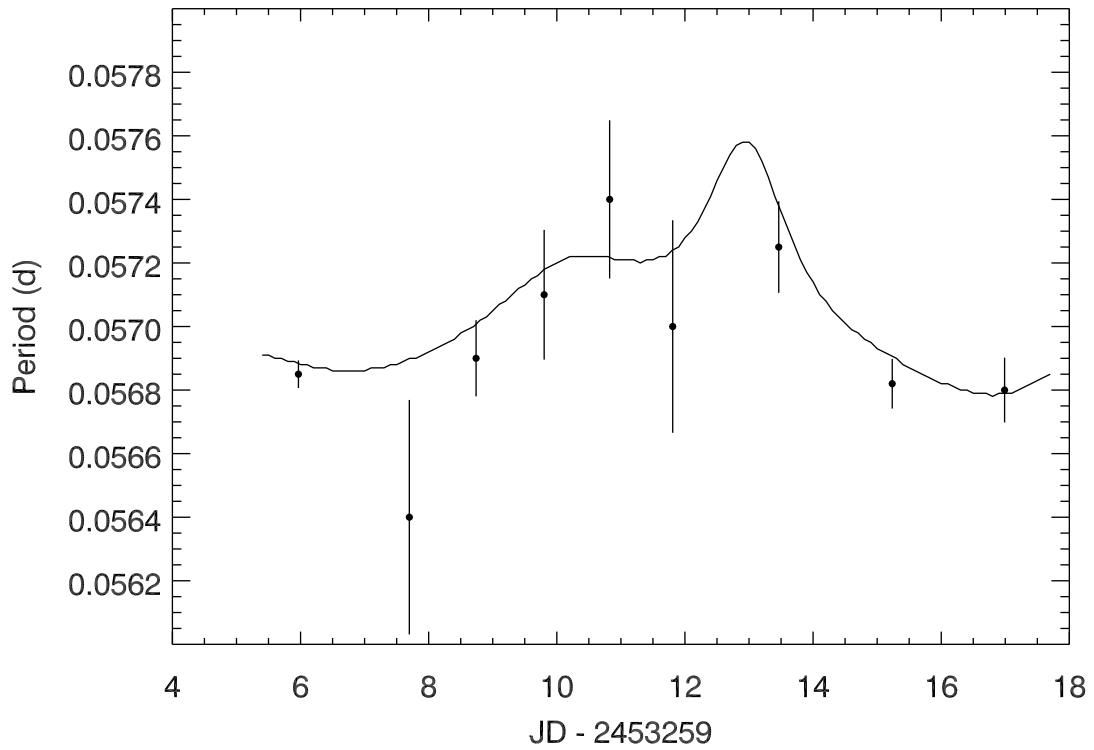


Fig. 3. | Period change in the superhumps during the early outburst. Points: periods derived from single days of photometry, with two-sigma error bars; solid line: period derived using the cluster analysis of Foster (1995). The period of the superhumps undergoes statistically significant period change beginning on the fifth day of photometry, approximately 8 days after the outburst was first detected.

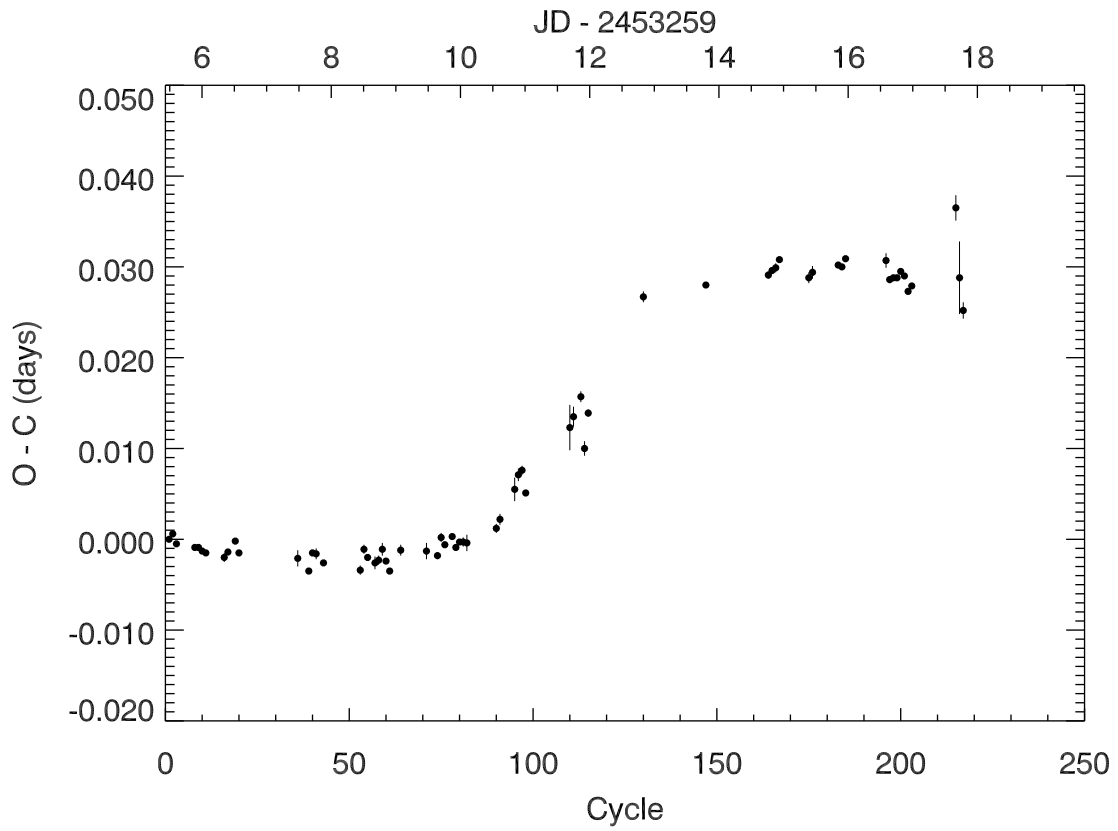


Fig. 4. | (O - C) diagram of the superhumps, assuming a period of 0.0569 days. There is a significant increase in period beginning at JD 2,453,272 before the superhumps return to the original period.

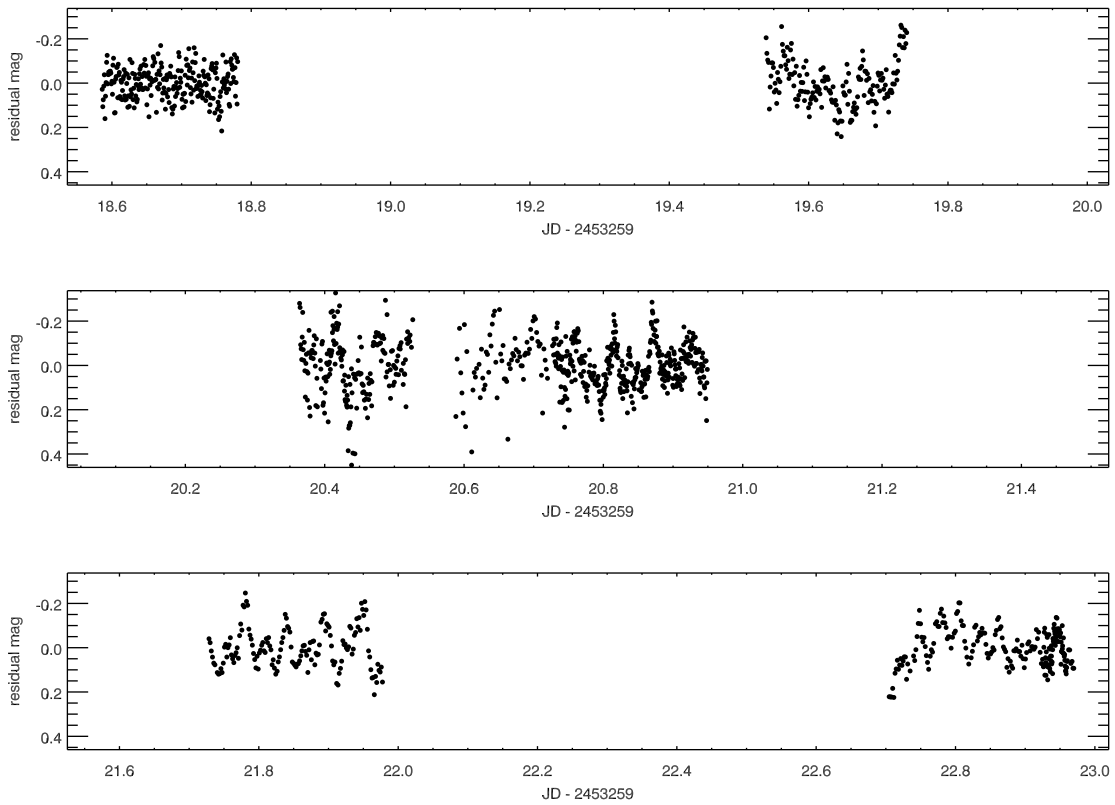


Fig. 5. | Detrended light curve showing the early decline period prior to the echo outburst. The profiles of the humps are qualitatively different from those of the superhumps observed during the superoutburst, and have a period of  $0.05666 \pm 0.00003$  days, below that of the late superhumps. We do not believe these are orbital variations.

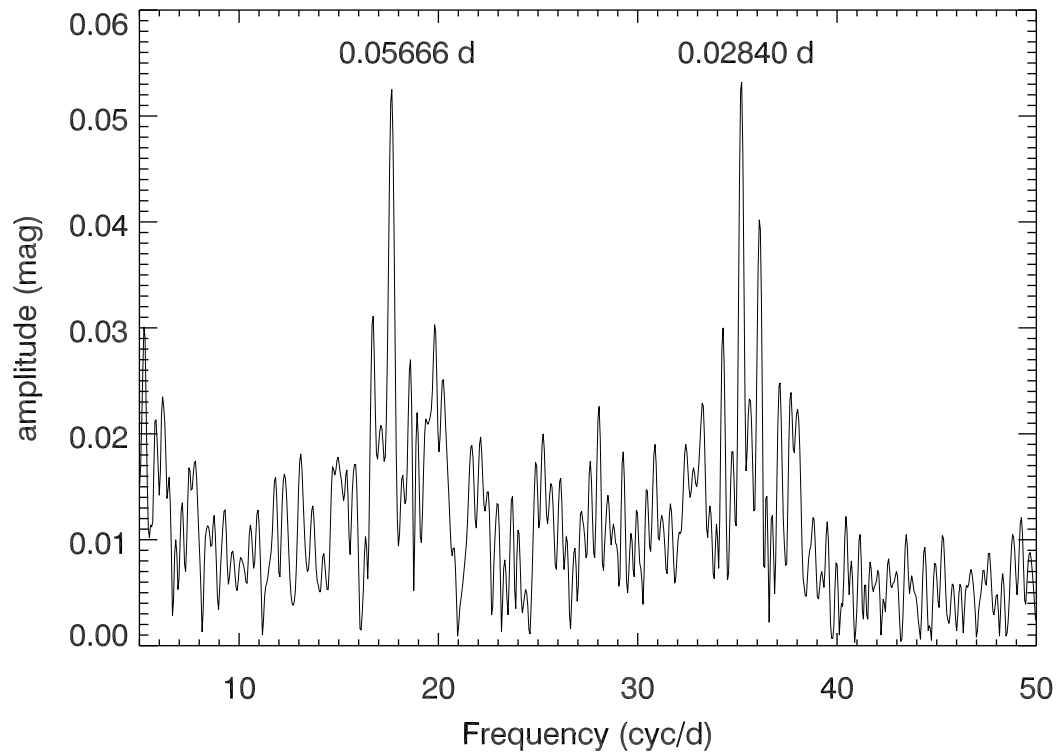


Fig. 6. | Discrete Fourier transform of the data shown in Figure 5, showing the period at 0.05666 days, along with its Fourier harmonic at half the period. The double-peaked nature of the light variations is explained by the nearly equal amplitudes of the two components.

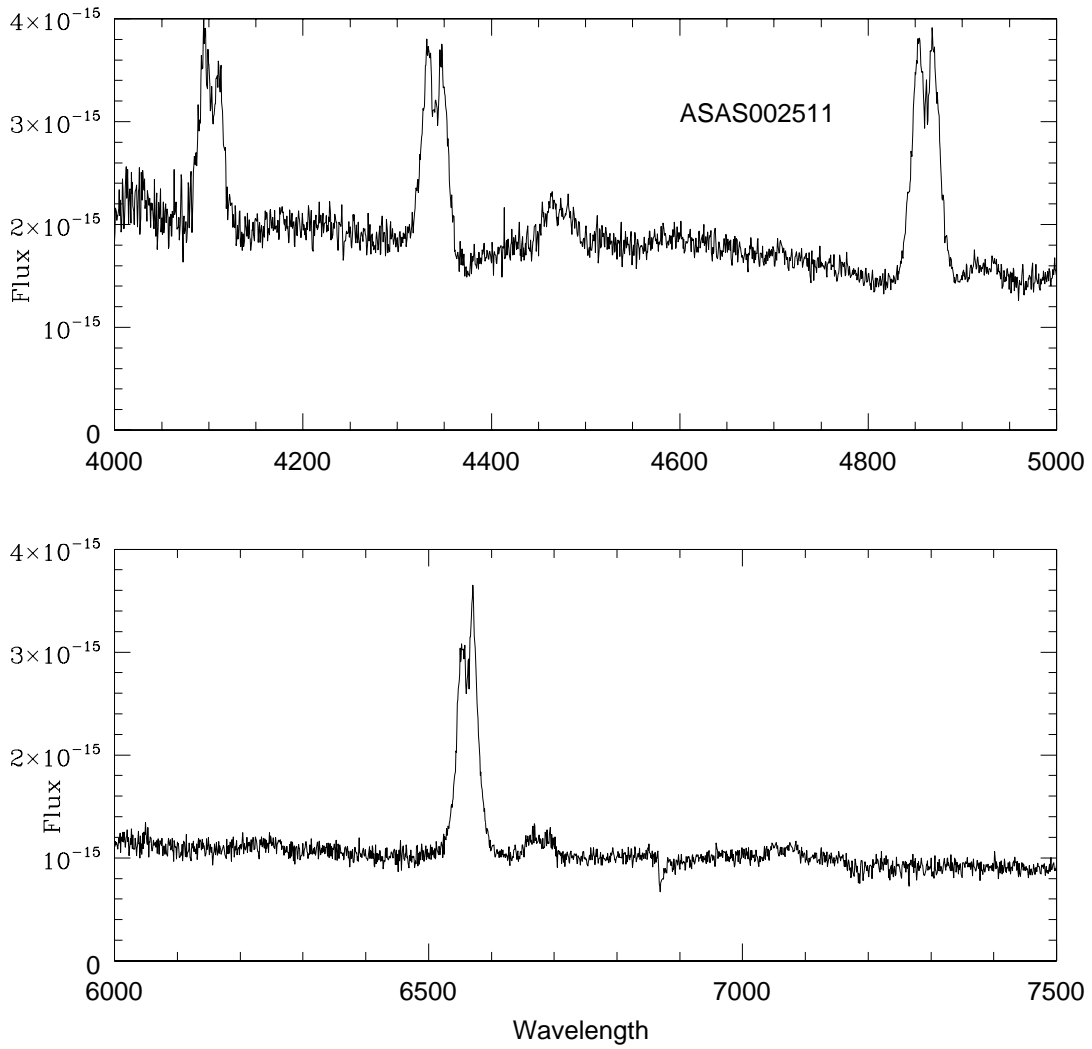


Fig. 7. | Typical blue and red spectra, showing the broad, double-peaked lines. The H $\gamma$  (6562.852 Å), H $\beta$  (4861.342 Å), and H $\delta$  (4340.475 Å) lines were all used for velocity measurements.

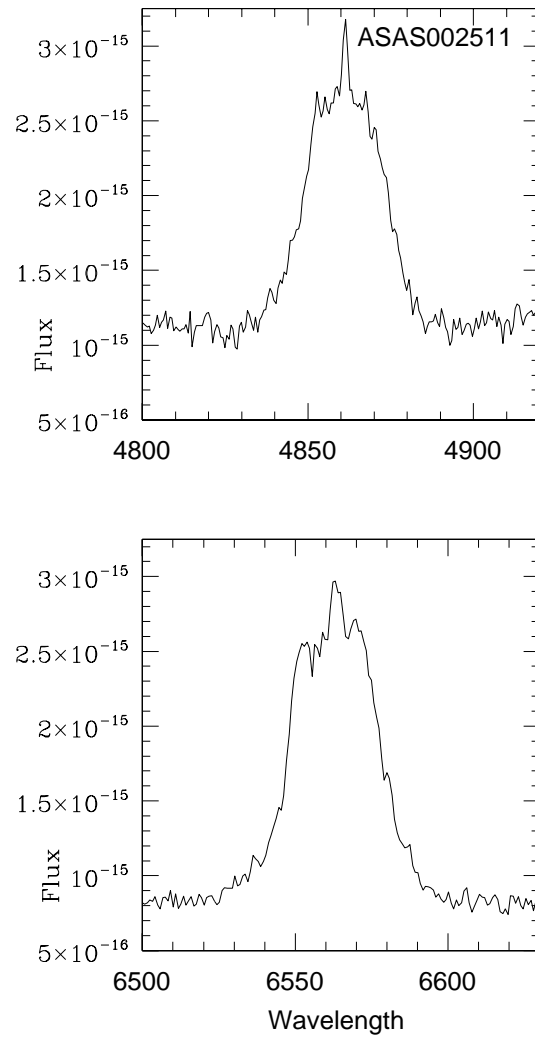


Fig. 8. | An enlargement of the H $\alpha$  and H $\beta$  lines at phase 0.9, showing the narrow component structure that is likely due to a hot spot on the outer edge of the accretion disk around the primary star.

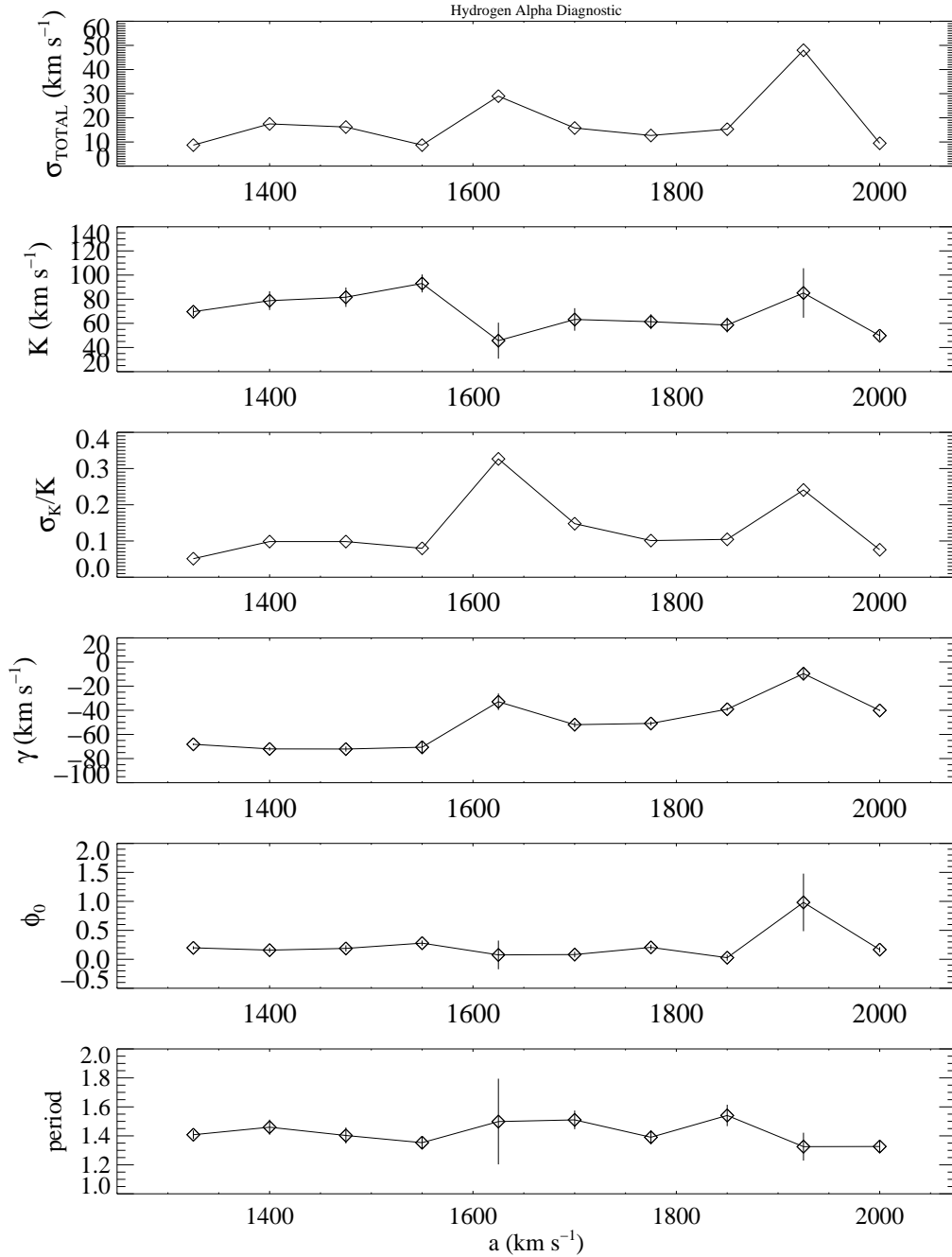


Fig. 9. | A sample diagnostic plot from the double Gaussian output. The velocities corresponding to a given double Gaussian separation are plotted with the characteristic parameters from the sinusoidal fit. For this H $\alpha$  line, a minimum  $\sigma_{\text{total}}$  corresponding to  $a = 1550 \frac{\text{km}}{\text{s}}$  was chosen.

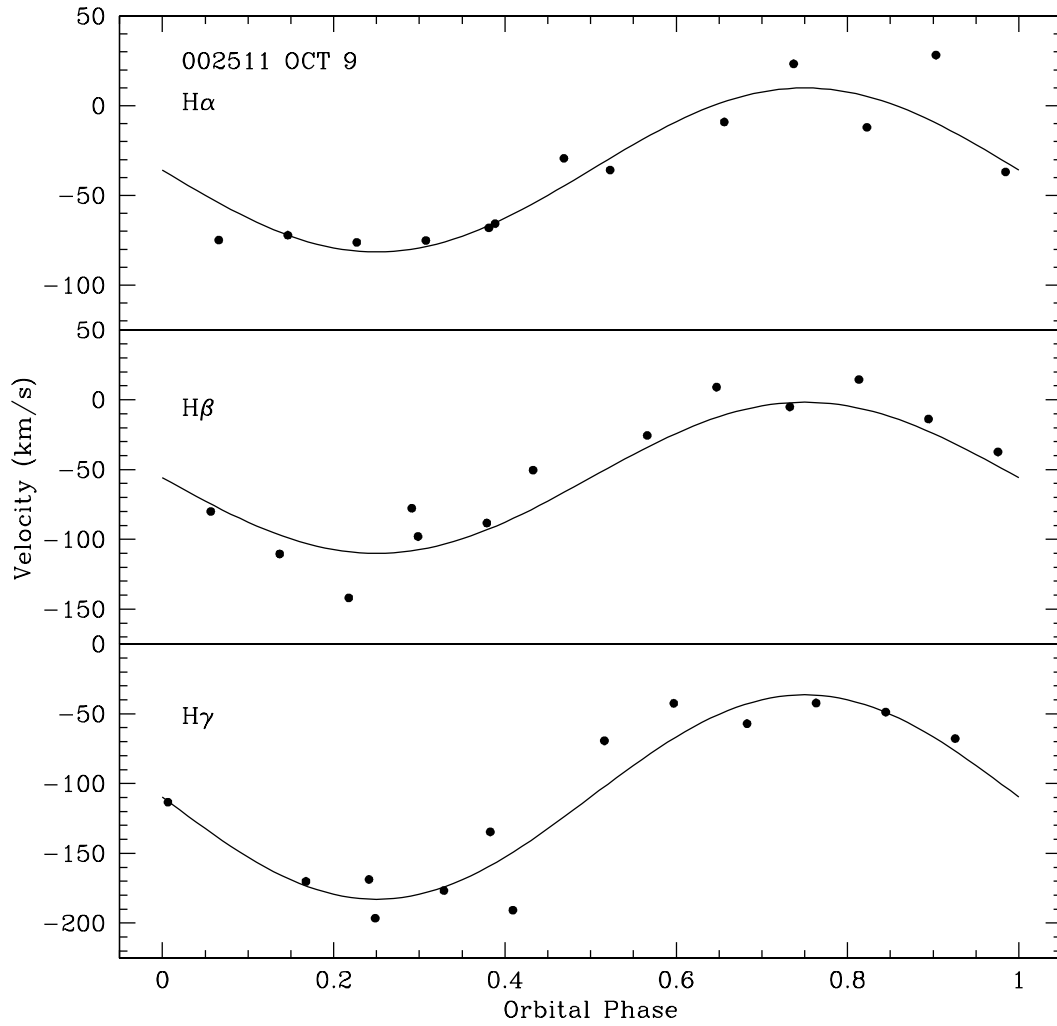


Fig. 10. The fits from the sinfit3 nal run are shown over-plotted on the velocity data points corresponding to the double Gaussian velocities with period fixed at 82 m in.

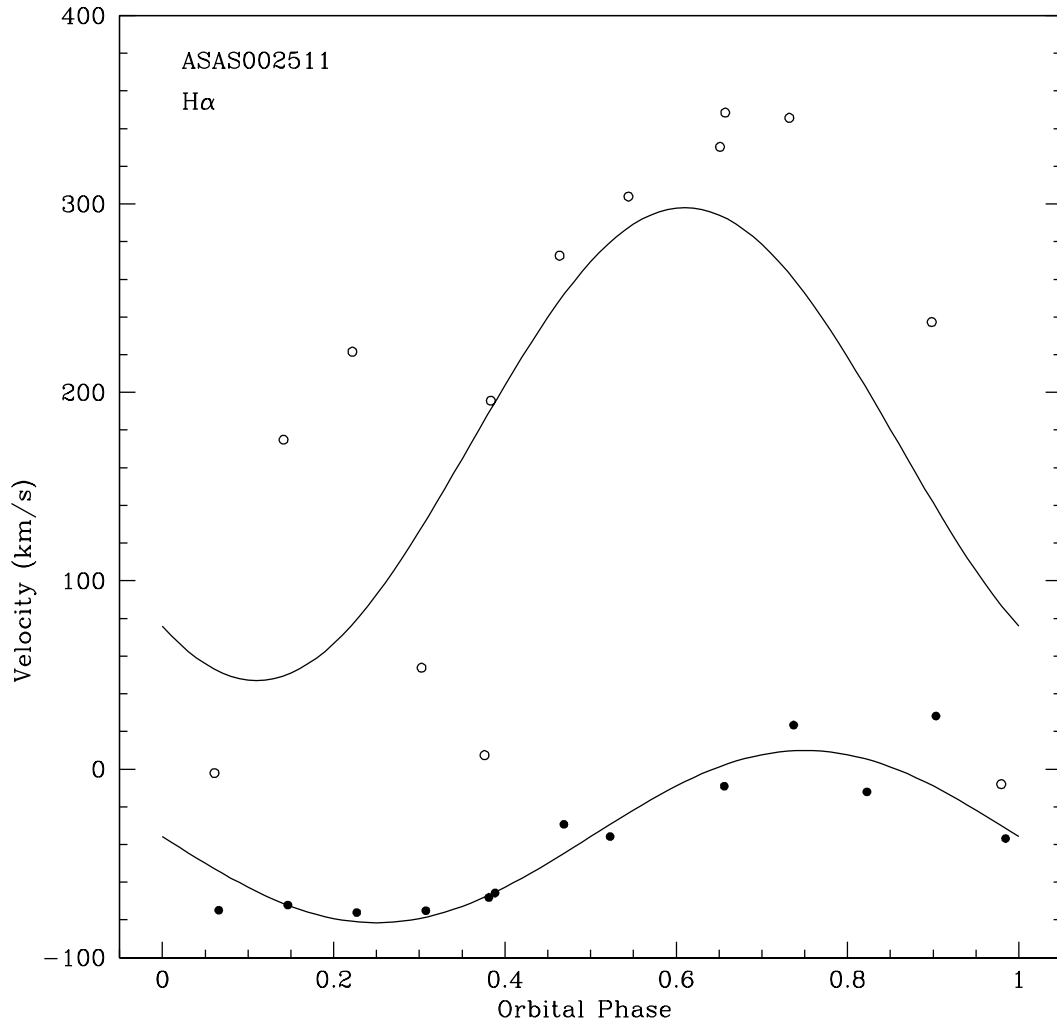


Fig. 11. Sinusoidal fit and data points for the narrow (open circles) and broad (filled circles) components of H $\alpha$ . Note the relative phase offset of the two components and the amplitude increase of the narrow component over that of the broad.

Table 1. Radial Velocity Solutions

Line Measurement Algorithm	Line	P (m in)	$p/P$ ( $\text{km s}^{-1}$ )	K ( $\text{km s}^{-1}$ )			0	total	
IrafCentroid	H	80.4	–	46	5	–36	1	0.17	14
	H	95.1	–	61	5	–55	1	–0.4	14
	H	91.1	–	78	5	–109	1	–0.2	14
Double Gaussian	H	81.2	0.03	93	7	–71	5	0.28	9
	H	83.9	0.09	41	9	–48	2	0.14	23
	H	80.2	0.08	50	2	–95	3	0.11	24
Double Gaussian	H	82	–	46	5	–36	1	0.1	14
	H	82	–	54	7	–56	1	0.2	19
Period fixed at 82	H	82	–	73	7	–110	2	0.2	20

Note. | Comparison of the radial velocity data using the two measurement algorithms discussed in the text. The final values should be taken from the last rows in the table.